Journal of Polymers and the Environment (2022) 30:1151–1161
https://doi.org/10.1007/s10924-021-02262-8

ORIGINAL PAPER

Enhanced Performance of *Aloe vera*-Incorporated Bacterial Cellulose/Polycaprolactone Composite Film for Wound Dressing Applications

Pornsuda Kotcharat[1] · Piyachat Chuysinuan[2] · Thanyaluck Thanyacharoen[2] · Supanna Techasakul[2] · Sarute Ummartyotin[1]

Accepted: 10 August 2021 / Published online: 22 August 2021

Abstract

Recently, biopolymers have become a resource for the biomedical material field due to its biocompatibility and biodegradability. In this work, *Aloe vera*-loaded bacterial cellulose- and polycaprolactone -based composites were successfully prepared for wound dressing applications. The structural, morphological, thermal, swelling, and degradation properties were investigated. Result showed that the addition of *Aloe vera* resulted in a strong peak characteristic of hydroxyl groups and amide I by attenuated total reflectance-Fourier transform infrared analysis. Pores were present inside the composite structure and varied with the *Aloe vera* content. No crystallinity peak of *Aloe vera* was observed. Thermogravimetric analysis indicated a slight change in the thermal decomposition temperature and a loss of water molecules below 100 °C. The swelling and weight loss behaviour were remarkably changed when only 5% *Aloe vera* was loaded into the composite. Moreover, *Aloe vera* enhanced the toughness and elongation of the composite. All the composites exhibited a burst release profiles within 60 min. The MTT assay showed a concerningly low cell viability concerning the amount of *Aloe vera* loaded into the composite. Therefore, *Aloe vera*-loaded BC and PCL composites could be developed for wound dressing applications.

Graphic Abstract

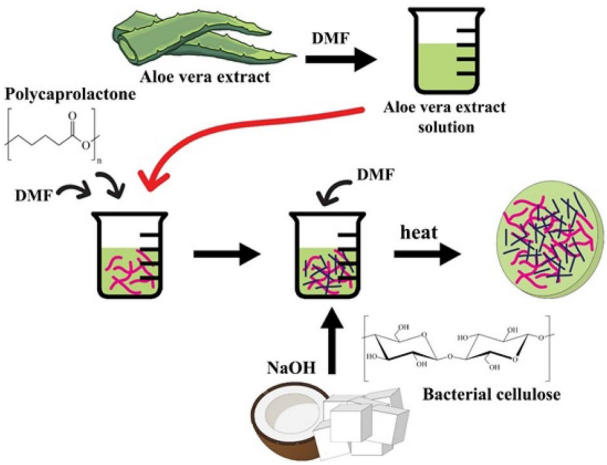

Keywords Bacterial cellulose · Polycaprolactone · *Aloe vera* · Composite

Introduction

In recent years, the exponential increase in numerous biomedical-based materials has been evident. Versatile biomedical materials have successfully been prepared for various

✉ Sarute Ummartyotin
sarute@tu.ac.th

Extended author information available on the last page of the article

medical sectors. There are common medical uses in various sectors, such as pharmaceutical technology, scaffolds in tissue engineering, wound repair and dental materials. Tissue engineering is an important application, as it provides many benefits, such as a novel strategy for medical therapy. Synthetic tissue acts as a biological alternative for the restoration and reconstruction of injured or diseased tissue. In general, it can create and control cell-cell and cell-substrate interactions. Therefore, the ideal tissue engineering material should be designed based on structure and functionality, as suggested by Luo et al. [1].

One of the most attractive biomedical materials is polycaprolactone. It exhibits high biocompatibility as well as optimal tensile strength. Furthermore, it exhibits excellent biodegradation behaviour, as reported by Abrisham et al. [2]. PCL holds great promise as a biomedical material due to its high resistance towards slip dislocation and fatigue. It can meet the crucial requirements for medical materials because it can overcome the limitations of ceramics. Moreover, the utilization of PCL in biomedical material has been authorized by the Food and Drug Administration's approval. It is safe for tissue engineering, as suggested by Harikrishnan et al. [3]. However, the research and development of PCL has been much improved to date. Bulbul et al. [4] developed a silane-modified halloysite clay nanotube-reinforced PCL-based composite. It was fabricated by electrospinning. The correlation between its morphological and mechanical properties was investigated by atomic force microscopy. Aydogdu et al. [5] developed graphene oxide and Fe_3O_4 filled into PCL-based composites by electrospinning. The biocomposite is promising for use as a scaffold in tissue engineering. The cell proliferation rates for 3T3 fibroblasts and Saos-2 osteosarcoma were reported to be 103% and 105%, respectively. Adhikari et al. [6] incorporated metallic magnesium particles into PCL nanofibre mesh to improve its biomedical properties. Magnesium significantly enhances tissue repair. Notably, the fibre was non-cytotoxic for 3T3 fibroblasts and PC-12 pheochromocytoma cells. The in vivo implantation under the skin of mice led to good vascularization after 28 days. Furthermore, Liao et al. [7] developed PCL and zein-calcium lactate composites for nonwoven mats by a two-nozzle electrospinning route. The presence of calcium lactate can effectively improve the mechanical properties, mineralization ability and biocompatibility. The in vivo test reported great promise for cell affinity.

To encourage the use of environmentally friendly materials, bacterial cellulose was included as an additive for the development of PCL-based biocomposites. Notably, BC was considered a nanodimensional network produced from the bacterial strain *Acetobacter xylinum*, as reported in many previous works [8–10]. It exhibited high thermal stability, high chemical resistance, and excellent mechanical properties. Therefore, inserting the BC network into a PCL composite effectively enhances the properties of pristine PCL. Recently, Figueiredo et al. [11] developed BC and PCL through a biosynthetic route. PCL powder was integrated into BC without a change in morphology. The composite had superior mechanical properties. Altun et al. [12] studied cells on the surface of BC and PCL. The composite illustrated optimal biocompatibility and consequently provided great promise for skin tissue engineering. Furthermore, Sepúlveda et al. [13] developed BC and PCL composites for rabbit corneal implants. The implants were employed as a physical barrier and provided biocompatibility to ocular cells. However, implantation prolonged the inflammation and collagen disorganization.

To the best of our knowledge, although PCL and its composite have been employed in various medical materials, they have low water absorption. This property limits their use. The design of scaffolds for the wound healing should be considered because wounds tend to have high moisture content and exhibit drastic swelling behaviour. The role of moisture content and swelling behaviour are key factors in the optimization of biochemical reactions that transferred proteins (growth factor/fibroblast/collagen) and expelled degenerating cells [14–16]. As a result, polycaprolactone effectively provides benefits for the cell adhesion and proliferation. *Aloe vera* is one of the most common naturally occurring medicinal plants, and it can improve moisture content and swelling behaviour. It is commonly utilized for treating skin trauma, such as burns and infections, and it provides moisture to the skin [17]. Transparent mucilaginous gel can be obtained from *Aloe vera* leaves. It has high water content of approximately 99%. These gels had glycoproteins and lectins that encourage cell regeneration and prevent wound inflammation [18, 19]. Recently, El-Sayed et al. [20] found that *Aloe vera* is an effective source of nutrients. *Aloe vera* pulp possesses excellent quantities of water-soluble vitamins such as (B1) 9.73 mg/g, (B2) 141.2 mg/g, and (B3) 4.63 mg/g along with a high content of maltose and fructose as disaccharides and galactose as monosaccharide. Moreover, the acemannan in *Aloe vera* is anti-inflammatory and antiviral properties, and it provides immune system stimulation [21]. Asthana et al. [22] developed an *Aloe vera* and polyvinyl alcohol-based composite membrane for skin care cosmeceutical products. It was used to heal the skin from various types of ailments. Bialik-Was et al. [23] evaluated the control-release mechanism of *Aloe vera* from sodium alginate and polyvinyl alcohol hydrogel composites. The kinetics of the release mechanism were evaluated for one week. Good results of a cell cytotoxicity test were observed for normal human dermal fibroblasts. Furthermore, the presence of *Aloe vera* in composites can be effectively induced to ease the degradation behaviour of enzymes, as reported by Pereira et al. [24]. For these

reasons, *Aloe vera* was employed to provide moisture and to act as an active agent to support the wound healing process in this work.

In this paper, *Aloe vera*-loaded BC and PCL-based composites for scaffold materials was developed. The physicochemical properties of the composite, such as the structural, thermal, and morphological properties, release characteristics, and swelling/degradation behaviour, were investigated. Cell cytotoxicity tests were also performed.

Experimental

Materials

Nata de coco syrup was purchased from Talad thai, Pathumthani, Thailand. Polycaprolactone (PCL) (MW 50,000) was purchased from Polyscience, Inc., USA. Sodium hydroxide was purchased from Sigma—Aldrich Co., Ltd., USA. *Aloe vera* powder was purchased from Chemipan Co., Ltd., Thailand. Analytical reagent-grade N,N-dimethylformamide (DMF) was purchased from Ajax Finechem Co., Ltd., Australia. All chemical reagents were used as received without further purification.

Methods

Bacterial Cellulose Extraction and Purification

BC was extracted from *nata de coco*, washed with distilled water to remove the syrup and blended in a laboratory blender. After that, *nata de coco* was treated with 2% w/v NaOH solution at 80 °C for 3 h to remove impurities. BC was cleansed with distilled water until a neutral pH was reached. After that, the BC suspension was filtered through vacuum suction filtration to obtain only the BC pellicle. The process of BC extraction was adjusted from our previous articles [9, 25, 26]. To prepare the composite, 1 wt% BC was suspended in DMF for 1 h.

Preparation of *Aloe vera*-Loaded BC and PCL-Based Composite Films

Aloe vera-loaded BC and PCL-based composites were prepared by casting onto a Petri dishes. First, 10 wt% PCL was completely dissolved in DMF. *Aloe vera* powder was also dissolved in DMF at 5%, 10%, 20%, and 30% by weight. After that, each *Aloe vera* solution was poured into a PCL solution and continuously stirred for 3 h at ambient temperature. Then, 20% v of BC suspension was poured into the *Aloe vera* and PCL mixture. The mixture was continuously stirred for 15 min at room temperature. Next, the solution was cast onto a Petri dish and then placed over a hot bath to remove the solvent. Then, the sample was dried at room temperature and stored in a desiccator to prevent moisture adsorption. A BC- and PCL-based composite film (AV0) was set as a control, whereas the *Aloe vera*-loaded BC and PCL-based composites at different concentrations were denoted AV5, AV10, AV20, and AV30.

Swelling Properties of *Aloe vera*-Loaded BC and PCL Composite Film

The swelling properties of the composite film were studied by using the gravimetric technique. The measurement was recorded as the weight of the sample before (W_{dry}) and after (W_{wet}) immersion in deionized water. After immersion in deionized water, the weight was recorded at each time point. The data are reported as statistical averages and standard deviations. The swelling ratio was determined as follows (Eq. 1).

$$\text{Swelling ratio } (\%) = (W_{wet} - W_{dry})/W_{dry} \times 100 \quad (1)$$

where W_{wet} is the weight of the swollen film at the end of submersion and W_{dry} is the initial weight of the dry film.

In vitro Degradation Behaviour

Each sample was cut to (1.5 × 1.5) cm. Then, the samples were immersed in 20 mL of phosphate buffer saline (PBS) solution at 37 °C for 4 weeks. They were removed from the solution and weighed at each time point after drying in an oven for 24 h. The percent degradation was calculated using (Eq. 2).

$$\text{Degradation } (\%) = \left(W_t/W_0\right) \times 100 \quad (2)$$

where W_0 is the weight before degradation and W_t is the weight after degradation.

In vitro Release Investigation

The *in vitro* release of *Aloe vera*-loaded BC/PCL film was investigated by using the immersion method. The samples were immersed in PBS (20 mL) solution at 37 °C for 48 h. At given intervals, 2 mL of *Aloe vera* solution was withdrawn, and an equal amount of original PBS with pH 7.4 was then added to maintain a constant volume. The release was measured, the absorbance at 260 nm was recorded using a microplate reader (BioTek Synergy H1, USA), and the cumulative release at various times was calculated according to the calibration curve. All values are reported as average ± standard deviation, and all experiments were conducted in triplicate.

Cytotoxicity Test

Cell cytotoxicity tests were conducted with the 3-(4,5-dimethylthiazol-2-yl)-2,5-diphenyltetrazolium bromide (MTT) cytotoxicity assay (based on ISO 10993-5) standard test method using L929 mouse fibroblast cells (ATCC CCL1, NCTC 929, strain L). L929 fibroblast cells cultivated in DMEM (Dulbecco's Modified Eagle Medium, Gibco, USA) were seeded into a 96-well plate (NUNC™, Thermo Scientific™, USA). The cells were incubated at 37 °C, 5% CO_2 and 95% relative humidity for 24 h to obtain a confluent monolayer of cells prior to testing. The blank was set as media without a test specimen. A Thermanox coverslip was used as a negative control, while a polyurethane film containing 0.1% zinc diethyldithiocarbamate (ZDEC) was employed as a positive control. The viable cells were stained with MTT and incubated for 2 h. The MTT was removed, and dimethyl sulfoxide was added to each well. The absorbance of the tested specimens was investigated using a microplate reader at a wavelength of 570 nm.

Characterization

Field Emission Scanning Electron Microscopy

The sample was investigated using scanning electron microscopy (SEM) (Quanta 250 microscope, Japan). The specimens were gold-coated using a sputtering device (Jeol, JFC-1200) prior to SEM observation. Magnification of 500 × and accelerating voltages of 1 kV were used.

Attenuated Total Reflectance-Fourier Transform Infrared (ATR-FTIR) Spectroscopy

The sample was investigated using ATR-FTIR analysis. The spectra were recorded using a Nicolet170- SX (Thermo Nicolet Ltd., USA) to detect the chemical composition of the samples. The wavenumber range was from 4000 to 100 cm^{-1}. A resolution of ± 4 cm^{-1} was set, and the number of scans was 32.

X-ray Diffraction

The crystal structure was investigated by X-ray diffraction (XRD, Bruker Model-D8 DISCOVER, Bruker, USA). It employed nickel filtered CuKα radiation. Diffraction patterns were recorded over a range of 15–30° with a scanning rate of 0.02°/min. Prior to the analysis, the sample was stored in a desiccator to prevent moisture absorption.

Thermogravimetric Analysis

Thermal degradation behaviour was characterized using thermogravimetric analysis (TGA, NETZSCH TG 209 F3 Tarsus®, Germany). The sample (20 mg) was heated from room temperature to 600 °C under nitrogen gas at heating and flow rates of 5 °C/min and 70 mL/min, respectively.

Mechanical Properties

Mechanical properties were tested by a Tinius Olsen H50KS universal testing machine. The specimen was cut into a length of 80 mm and a width of 10 mm. The crosshead speed was set at 5 mm × min^{-1} under a 50 kN load cell. The results, such as tensile strength, elongation at break and Young's modulus, were reported as a statistical average of five samples.

Results and Discussion

An *Aloe vera*-loaded BC and PCL composite was successfully prepared. The composite presented as a flat sheet and whitish colour. The FTIR spectra of the *Aloe vera*-loaded BC and PCL composite are presented in Figure 1. The spectrum of the pristine composite was provided for comparison. The variation in the amount of *Aloe vera* load in the composite was evaluated based on structural properties. The characteristic peaks of PCL at 2864 and 2949 cm^{-1} were attributed to symmetric and asymmetric C-H stretching, respectively. The presence of a characteristic peak at 1726 cm^{-1} is attributed to carbonyl stretching. The characteristic peak at 1296 cm^{-1} is typically due to C-O and C–C stretching in the backbone

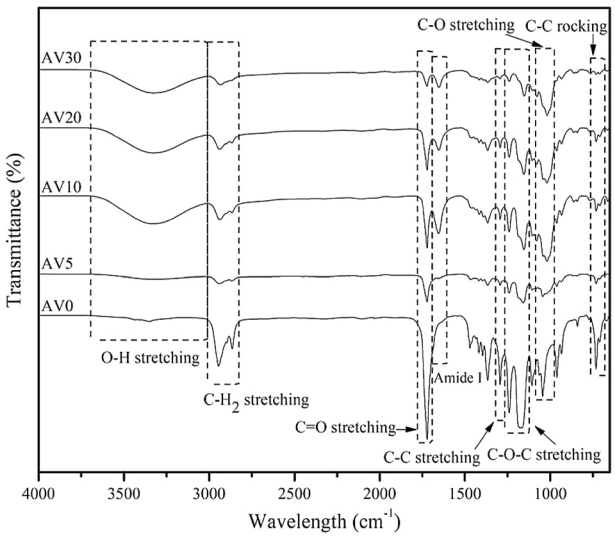

Fig. 1 FTIR spectra of the *Aloe vera*-loaded BC and PCL composite

of the crystalline phase. Moreover, the presence of characteristic peaks at 1175 and 730 cm^{-1} correspond to C–O–C stretching and backbone C–C rocking, respectively. These results are in agreement with those of the previous work of Elzein et al. [27]. However, the characteristic peak of neat BC was not evident. The FTIR spectra of all composites were identical to that of pristine PCL. This result confirmed that a high amount of PCL was present as a matrix phase in the composite. To investigate the functional group of *Aloe vera*, the determination of the acetyl group was necessary for biological activation, as suggested by Abdel-Mohsen et al. [28]. The presence of a broad peak at 3316 cm^{-1} was attributed to O–H stretching. This peak was due to carbohydrate monomers in the *Aloe vera*, such as uronic acid, mannose or galacturonic acid, or phenolic compounds such as aloin and aloe-emodin [29]. The peak at 1657 cm^{-1} was associated with C = O, related to a characteristic amide I group [30]. The characteristic peak at 1025 cm^{-1} represented C-O stretching related to rhamnogalacturonan, which is a side chain of pectin. This result was similar to the results of previous work reported by Lim et al. [31]. On the one hand, the spectrum of the *Aloe vera*-loaded BC and PCL composite presented all characteristic peaks with different absorption. The increase in the *A loe vera* content in the composite increased the intensity of the peak at 3323 cm^{-1}. On the other hand, the intensity of PCL peaks was reduced. A possible explanation is that the absorption band of *Aloe vera* obscured the characteristic peak of PCL, as suggested by Ghorbani et al. [32]. Moreover, the absorption band of *Aloe vera* was affected by the characteristic peak of the composite, as the sharp peak changed to a broad peak.

To evaluate the presence of BC in the PCL composite, the morphological and homogeneous properties of the composite were reported. Figure 2 illustrates a cross-sectional view of the *Aloe vera*-loaded BC and PCL composite. The pristine composite is provided for comparison. The distribution of BC in the PCL matrix was considered an important key because it can strongly affect the performance of the composite, as suggested by Kalita et al. [33]. Notably, PCL filled the porous network of BC nanofibers and consequently generated in the compact composite. However, the presence of voids inside the composite was also observed. These voids were probably due to the evaporation of solvent during BC and PCL composite preparation. The microstructure of the composite was typically observed. No considerable change in morphology was observed. The phase separation between the BC and PCL was not observed when the percentage of *Aloe vera* was increased. However, a high amount of *Aloe vera* can lead to porosity inside the composite structure. It behaves as a close cellular foam in the composite. A low evaporation rate of solvent can create a small pore size inside the composite, whereas a fast evaporation rate can create a large pore size. Thus, the solvent should be removed during preparation. The close cellular foam can effectively provide the ability of the *Aloe vera*-loaded BC and PCL composite is employed as a wound dressing material due to its cell adhesion and control-release rate. This result was strongly aligned with the previous literature by Hassan et al. [34].

To evaluate the crystal structure of the *Aloe vera*-loaded BC and PCL composite, XRD technique was employed. Figure 3 exhibits the XRD pattern of *Aloe vera*-loaded BC and PCL composite. The XRD pattern of the neat composite was provided for comparison. Characteristic peaks observed at 2θ values of 21°, 22° and 24° corresponded to diffraction planes of (110), (111), and (200), respectively. These three sharp peaks corresponded to PCL, similar to Baptista et al. [35]. However, due to the small amount of bacterial cellulose, diffraction peaks could not be observed. To the best of our knowledge, BC presented the main characteristic peaks at 2θ angles of 14°, 17° and 23° [36]. Furthermore, when the *Aloe vera* molecule was loaded into the BC and PCL composite, no remarkable peak was observed probably due to the low amount of *Aloe vera* added. Alternatively, it may have occurred because the *Aloe vera* became embedded in the close cellular foam of the composite that may have led to a decreasing in the crystallinity of the composite.

The thermal degradation behaviour of *Aloe vera*-loaded BC and PCL composites was determined by TGA. Figure 4 presents the TGA curve of the thermal decomposition of *Aloe vera*-loaded BC and PCL composite. The thermal decomposition of the pristine composite began at 76 °C with a mass loss of approximately 2%. The mass loss was due to the evaporation of water and moisture. Next, 98% weight loss occurred at 326–490 °C due to the decomposition of the BC and PCL composite. In the case of the *Aloe vera* loaded composite, the weight loss of the composite occurred in three steps. The first region of weight loss was found in the temperature range of 50–156 °C. The weight of the samples decreased by approximately 2%–26% up to the concentration of *Aloe vera*. These results were related to the evaporation of water and solvent inside the composite structure. Then, the second region of weight loss was exhibited at 156–335 °C. It was involved in the thermal degradation of *Aloe vera,* as reported by Khor et al. [37]. Furthermore, the final region of weight loss started at 366 °C. This weight loss may be related to the decomposition of the BC and PCL composite. The presence of *Aloe vera* resulted in a decrease in its thermal stability. Moreover, the concentration of *Aloe vera* in the composite was associated with weight loss behaviour at temperatures lower than 150 °C. When the concentration of *Aloe vera* was high, it presented weight loss superior to that of the other sample. This phenomenon is due to the hydrophilicity of *Aloe vera,* which maintains water and solvent inside the composite film. This result was in agreement with that of the previous work of Bajer et al. [29].

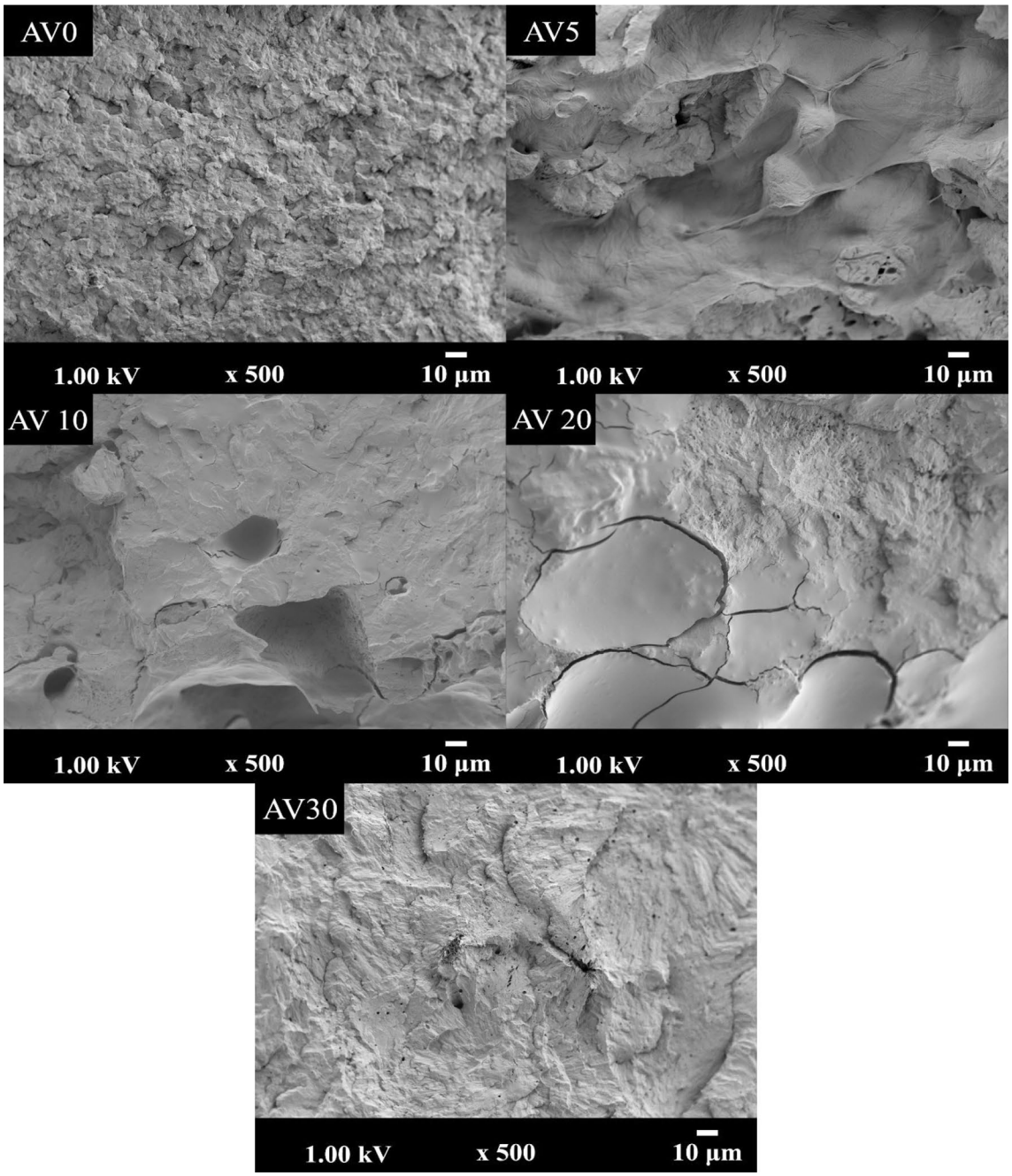

Fig. 2 Morphological characterization of the *Aloe vera*-loaded BC and PCL composite

Swelling behaviour is considered an important characteristic of wound dressing materials. The role of swelling behaviour can determine the capacity of composites to absorb exudates from wounds, for gas exchange, and for cell attachment [38]. Furthermore, it can be employed to evaluate the kinetic mechanism of drug release through osmosis, as suggested by Anbazhagan et al. [39]. Figure 5 exhibits the swelling behaviour of the *Aloe vera*-loaded BC and PCL composite film in deionized water. The BC and composite without *Aloe vera* presented inferior water absorption compared to the *Aloe vera* composite. This result is due to the hydrophobic properties of PCL that was the matrix phase in the composite. Moreover, the composite presented a low porous structure that affected the permeability of water into the composite structure. This result was similar to that of the previous work of Zahedi et al. [40]. In the case of the *Aloe vera* loaded composite, the water absorption was substantially enhanced. This enhancement was related to the

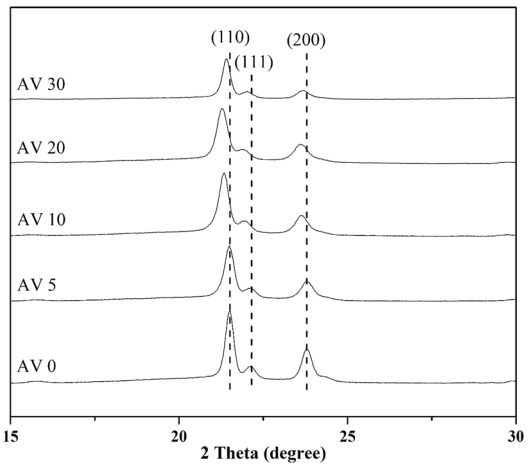

Fig. 3 XRD pattern of the *Aloe vera*-loaded BC and PCL composite

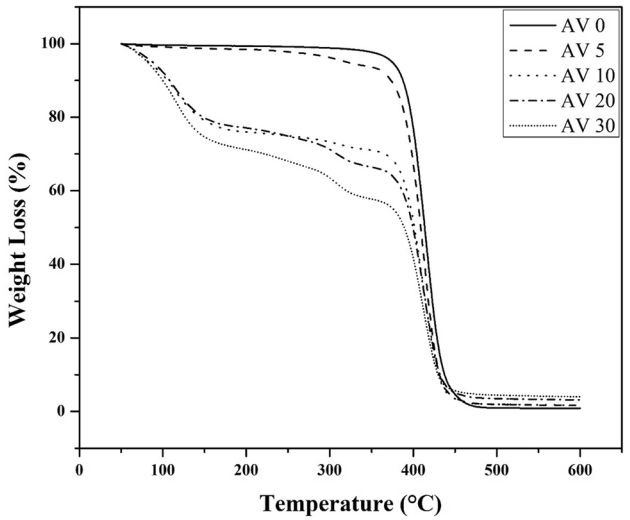

Fig. 4 Thermal decomposition behaviour of the *Aloe vera*-loaded BC and PCL composite

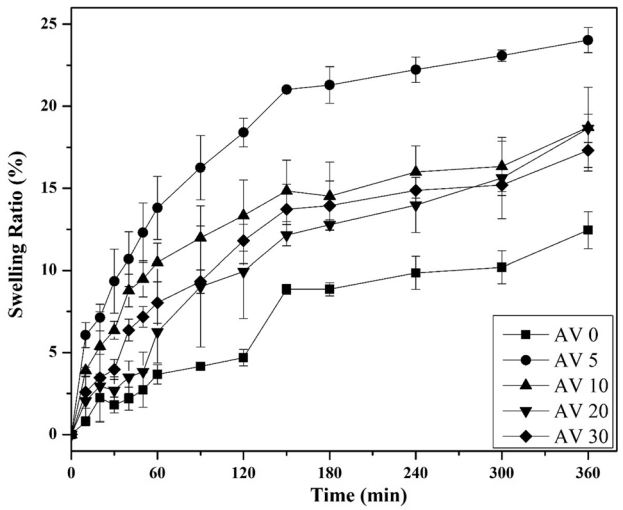

Fig. 5 Swelling behaviour of the *Aloe vera*-loaded BC and PCL composite

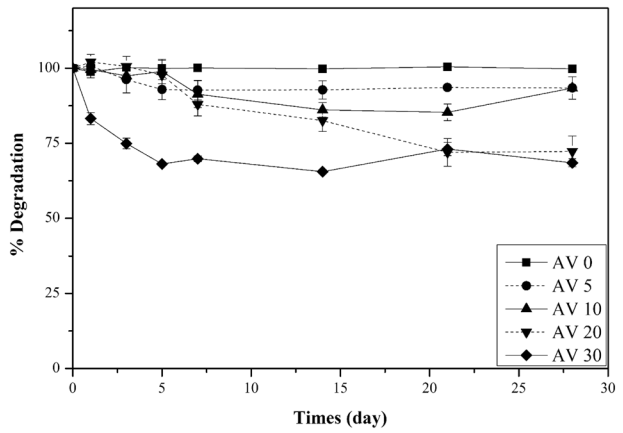

Fig. 6 In vitro degradation behaviour of *Aloe vera*-loaded BC and PCL composite in PBS medium

high quantity of O–H groups in the chemical structure of *Aloe vera,* which induce water into the structure, as reported by Pereira et al. [41]. This explanation is supported by the SEM microstructure investigation shown in Figure 2. The porosity and cracks between the BC/PCL interface allowed water molecules to diffuse into the structure, as suggested by Shayuti et al. [42]. In contrast, although the high porosity of the composite enhanced the swelling properties, it accelerated the weight loss of the composite when a high amount of *Aloe vera* was loaded.

To use *Aloe vera*-loaded BC and PCL composite as a scaffold material, the *in vitro* degradation behaviour was observed. The measurement of the statistical average weight loss was key to evaluating the efficiency of the scaffold degradation. Schindler et al. [43] stated that in vitro degradation was desirable for applications such as tissue regeneration and drug delivery to retain the mechanical properties of the composites during the reconstruction and the release of drug molecules. Figure 6 presents the percentage of weight loss of *Aloe vera*-loaded BC and PCL composite versus incubation time. The pristine composite was provided for comparison. The experiment was set up for 28 days at ambient temperature. The degradation behaviour of the pristine composite was low. Only 2 wt% weight loss was observed over the whole experiment. The BC did not lead to weight loss in the composite because of the low amount. Additionally, the cellulose was embedded into the PCL matrix. The weight loss behaviour was probably only due to PCL. It is a hydrophobic crystalline polymer, and thus, water molecules do not easily penetrate it. This observation strongly agreed with

the results of a previous report by Melnik et al. [44]. By contrast, when *Aloe vera* was loaded into the composite, weight loss was observed. The range of weight loss was observed to be 5%–25% depending on the amount of *Aloe vera*. The percent weight loss was stable over the incubation period. The *in vitro* degradation behaviour was accompanied by the release of *Aloe vera* molecules into the PBS solution. This release of molecules can enhance osteoconduction when the composites are employed as scaffold materials, as suggested by Ghorbani et al. [32].

The mechanical properties of *Aloe vera*-loaded BC and PCL composites were measured. Table 1 presents the tensile strength, % elongation at break and Young's modulus of the composite. The pristine composite exhibits high tensile strength and Young's modulus compared to the *Aloe vera*-loaded composite. The interaction between BC and PCL occurred in the composite network, as suggested by Aydogdu et al. [45]. This interaction can disrupt the chain slippage, which subsequently deforms the composite structure. Additionally, it is important to note that the presence of *Aloe vera* can provide a high percent of elongation at break. It can create a heterocyclic complex among BC and PCL networks. This result was similar to the results reported in the previous literature of Carter et al. [46]. Furthermore, the porosity could improve the tensile strength and percent elongation at break. This improvement may be related to the diameter of the interpore in the composite structure. When the interpore diameter decreased, it tends to lose interpore stiffness. This observation was in agreement with those reported by Zeleniakiene et al. [47]

The *in vitro* drug release profile was considered a simulation technique to determine the control-release mechanism of wound dressing material. Figure 7 shows the *in vitro* release profile of *Aloe vera*-loaded BC and PCL composites. All composites presented burst release effects in the first interval of investigation, and the release rate slightly increased from 20 to 2880 min. The amount of *Aloe vera* loaded into the composite influenced the release profile. Within 1 h, a high release rate was observed due to the fast diffusion of *Aloe vera* molecules from the surface of the composite, and then the *Aloe vera* diffused from the inside,

Table 1 Mechanical properties of the *Aloe vera*-loaded BC and PCL composite

Sample	Tensile Strength (MPa)	% Elongation at break (%)	Young's modulus (MPa)
AV 0	47.9 ± 4.5	4.0 ± 4.4	3773.3 ± 11.5
AV 5	0.9 ± 0.5	12.0 ± 8.8	67.9 ± 1.1
AV 10	0.5 ± 0.1	13.1 ± 4.6	12.1 ± 7.2
AV 20	0.9 ± 0.2	13.0 ± 2.6	26.7 ± 5.4
AV 30	1.7 ± 0.6	8.1 ± 1.4	73.8 ± 2.5

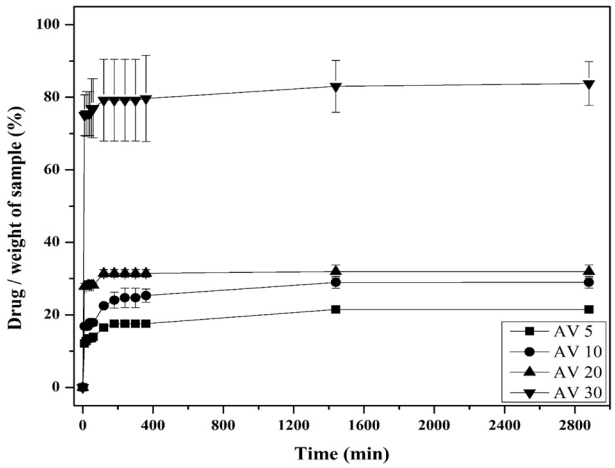

Fig. 7 *In vitro* drug release of the *Aloe vera*-loaded BC and PCL composite in PBS medium

as suggested by Siboro et al. [48]. The high release rate was due to the porosity inside the BC and PCL composite network. The porosity caused the *Aloe vera* to leak out, and the PBS medium easily diffused into the composite. When the *Aloe vera* content is high, the sample was likely to present hydrophilic character and high solubility. The *Aloe vera* can interact with the aqueous phase and consequently diffuse outside. Burst release was observed in the initial stage. This observation was similar to that in the previous work of Isfahnani et al. [49]. After the initial stage, the release rate was constant.

An MTT assay was employed to evaluate the biocompatibility of the *Aloe vera*-loaded BC and PCL composite. To achieve the ideal wound dressing, the material should promote cell attachment and cell proliferation, and it should be nontoxic. Figure 8 shows the percentage of cell viability of L929 mouse fibroblast cells on the *Aloe vera*-loaded BC and PCL composite. After 3 days of

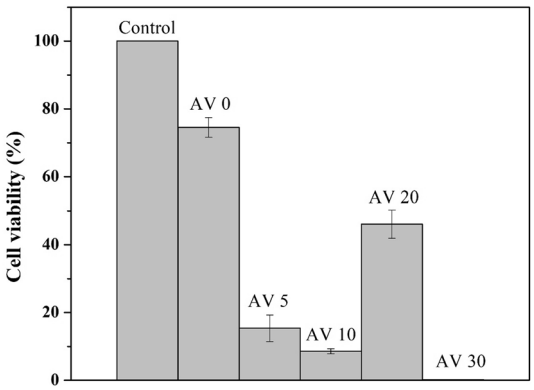

Fig. 8 The cell cytotoxicity test of the *Aloe vera*-loaded BC and PCL composite for 3 days

investigation, only the 30%wt. *Aloe vera*-loaded composite did not demonstrate cell viability, and the other samples exhibited cell viability inferior to that without *Aloe vera*-loading. This result implies that the amount of *Aloe vera* influences cell viability. Notably, high *Aloe vera*-loading can cause an extremely hydrophilic surface in the composite. It creates large repulsive forces between proteins and the layers of water or aqueous phase. As a consequence, it can lead to lower protein absorption, as suggested by Song et al. [50] and Ramos et al. [51]. However, DMF, which was employed as a solvent to prepare the composite, is harmful to cells and inhibits cell proliferation [52]. In the case of a high *Aloe vera*-loaded composite, the pores acted as reservoirs to store DMF inside the composite structure. When the sample was immersed in cell culture medium, the solvent diffused and caused damage to the cell. This result was consistent with the previous work of Li et al. [53].

Conclusion

In this paper, an *Aloe vera*-loaded BC and PCL composite was successfully prepared through solvent evaporation. The FTIR spectrum showed an incremental increase in transmittance when the *Aloe vera* content was increased. The SEM microstructure exhibited microcracks and porosity when *Aloe vera* was loaded into the composite. The amorphous phase of the *Aloe vera* hindered the crystalline phase of the PCL, that affected the tensile strength of the composite film. When only 5% *Aloe vera* was loaded into the composite, and the swelling and weight loss increased compared to that of the pristine composite. The release profile exhibited burst release at the first interval of investigation and become steady after 1 h of investigation. Although the *Aloe vera* loaded the composite presented excellent swelling behaviour and kinetic release rate, the cell cytotoxicity measured by an MTT assay illustrated a low cell viability, resulting from the *Aloe vera* content and the solvent from the composite preparation. To employ *Aloe vera*-loaded composites with higher efficiency, more attention should be given to the amount of *Aloe vera* and its solubility. Therefore, *Aloe vera*-loaded BC and PCL composites have great potential as ideal wound dressings.

Supplementary Information The online version contains supplementary material available at https://doi.org/10.1007/s10924-021-02262-8.

Acknowledgements This work was financially supported by the Thailand Science Research and Innovation (TSRI), Chulabhorn Research Institute (Grant No. 313/2229) and the Thammasat University Research Unit in Textile and Polymer Chemistry.

References

1. Luo J et al (2018) 3-D mineralized silk fibroin/polycaprolactone composite scaffold modified with polyglutamate conjugated with BMP-2 peptide for bone tissue engineering. Colloids Surf B 163:369–378
2. Abrisham M et al (2020) The role of polycaprolactone-triol (PCL-T) in biomedical applications: A state-of-the-art review. Eur Polym J 131:109701
3. Harikrishnan P, Sivasamy A (2020) Preparation, characterization of Electrospun Polycaprolactone-nano Zinc oxide composite scaffolds for Osteogenic applications. Nano Struct Nano Obj 23:100518
4. Bulbul YE et al (2020) Investigation of nanomechanical and morphological properties of silane-modified halloysite clay nanotubes reinforced polycaprolactone bio-composite nanofibers by atomic force microscopy. Polym Test 92:106877
5. Aydogdu MO et al (2018) Novel electrospun polycaprolactone/graphene oxide/Fe3O4 nanocomposites for biomedical applications. Colloids Surf B 172:718–727
6. Adhikari U et al (2019) Embedding magnesium metallic particles in polycaprolactone nanofiber mesh improves applicability for biomedical applications. Acta Biomater 98:215–234
7. Liao N et al (2016) Fabrication, characterization and biomedical application of two-nozzle electrospun polycaprolactone/zein-calcium lactate composite nonwoven mat. J Mech Behav Biomed Mater 60:312–323
8. Ummartyotin S et al (2012) Development of transparent bacterial cellulose nanocomposite film as substrate for flexible organic light emitting diode (OLED) display. Ind Crops Prod 35(1):92–97
9. Sakwises L, Rodthongkum N, Ummartyotin S (2017) SnO2- and bacterial-cellulose nanofiber-based composites as a novel platform for nickel-ion detection. J Mol Liq 248:246–252
10. O-Rak, K., et al (2014) Development of bacterial cellulose and poly(vinylidene fluoride) binary blend system: Structure and properties. Chem Eng J 237:396–402
11. Figueiredo ARP et al (2015) In situ synthesis of bacterial cellulose/polycaprolactone blends for hot pressing nanocomposite films production. Carbohyd Polym 132:400–408
12. Altun E et al (2019) Cell studies on Electrohydrodynamic (EHD)-3D-bioprinted Bacterial Cellulose\Polycaprolactone scaffolds for tissue engineering. Mater Lett 234:163–167
13. Sepúlveda R et al (2016) Bacterial cellulose and bacterial cellulose/polycaprolactone composite as tissue substitutes in rabbits' cornea. Pesqui Vet Bras 36:986–992
14. Scott C et al (2020) Adapting resistive sensors for monitoring moisture in smart wound dressings. Curr Opin Electrochem 23:31–35
15. Satish A et al (2019) Triiodothyronine impregnated alginate/gelatin/polyvinyl alcohol composite scaffold designed for exudate-intensive wound therapy. Eur Polymer J 110:252–264
16. Junker J et al (2013) Clinical impact upon wound healing and inflammation in moist, wet, and dry environments. Adv Wound Care 2:348–356
17. Tummalapalli M et al (2016) Composite wound dressings of pectin and gelatin with *Aloe vera* and curcumin as bioactive agents. Int J Biol Macromol 82:104–113
18. Das S et al (2011) Isolation and characterization of novel protein with anti-fungal and anti-inflammatory properties from *Aloe vera* leaf gel. Int J Biol Macromol 48(1):38–43
19. Ghayempour S, Montazer M, Rad MM (2016) Encapsulation of *Aloe vera* extract into natural Tragacanth Gum as a novel green wound healing product. Int J Biol Macromol. 93(Pt A):344–349

20. El-Sayed SM, El-Sayed HS (2020) Production of UF-soft cheese using probiotic bacteria and *Aloe vera* pulp as a good source of nutrients. Ann Agric Sci 65(1):13–20
21. Ahlawat K, Khatkar B (2014) Processing, food applications and safety of *Aloe vera* products: A review. J Food Sci Technol 48:525–533
22. Asthana N et al (2020) Polyvinyl alcohol (PVA) mixed green–clay and *Aloe vera* based polymeric membrane optimization: Peel-off mask formulation for skin care cosmeceuticals in green nanotechnology. J Mol Struct. https://doi.org/10.1016/j.molstruc.2020.129592
23. Bialik-Wąs K et al (2020) Advanced SA/PVA-based hydrogel matrices with prolonged release of *Aloe vera* as promising wound dressings. Mater Sci Eng C. https://doi.org/10.1016/j.msec.2020.111667
24. Pereira RF et al (2013) Influence of *Aloe vera* on water absorption and enzymatic in vitro degradation of alginate hydrogel films. Carbohyd Polym 98(1):311–320
25. Chunshom N et al (2018) Dried-state bacterial cellulose (Acetobacter xylinum) and polyvinyl-alcohol-based hydrogel: An approach to a personal care material. J Sci Adv Mater Dev 3(3):296–302
26. Phutanon N et al (2019) Development of CuO particles onto bacterial cellulose sheets by forced hydrolysis: A synergistic approach for generating sheets with photocatalytic and antibiofouling properties. Int J Biol Macromol 136:1142–1152
27. Elzein T et al (2004) FTIR study of polycaprolactone chain organization at interfaces. J Colloid Interface Sci 273(2):381–387
28. Abdel-Mohsen AM et al (2020) Chitosan-glucan complex hollow fibers reinforced collagen wound dressing embedded with aloe vera. Part I: Preparation and characterization. Carbohydr Polym 230:115708
29. Bajer D, Janczak K, Bajer K (2020) Novel Starch/Chitosan/Aloe vera composites as promising biopackaging materials. J Polym Environ 28(3):1021–1039
30. Fardsadegh B, Jafarizadeh H (2019) *Aloe vera* leaf extract mediated green synthesis of selenium nanoparticles and assessment of their In vitro antimicrobial activity against spoilage fungi and pathogenic bacteria strains. Green Process Synth 8:399–407
31. Lim ZX, Cheong KY (2015) Effects of drying temperature and ethanol concentration on bipolar switching characteristics of natural *Aloe Vera*-based memory devices. Phys Chem Chem Phys. https://doi.org/10.1039/c5cp04622j
32. Ghorbani M, Nezhad-Mokhtari P, Ramazani S (2020) *Aloe vera*-loaded nanofibrous scaffold based on Zein/Polycaprolactone/Collagen for wound healing. Int J Biol Macromol 153:921–930
33. Kalita NK et al (2020) End-of-life evaluation and biodegradation of Poly(lactic acid) (PLA)/Polycaprolactone (PCL)/Microcrystalline cellulose (MCC) polyblends under composting conditions. Chemosphere 247:125875
34. Hassan AA et al (2021) Polycaprolactone based electrospun matrices loaded with Ag/hydroxyapatite as wound dressings: Morphology, cell adhesion, and antibacterial activity. Int J Pharma 593:120143
35. Baptista C et al (2020) The effect of temperature and pressure on polycaprolactone morphology. Polymer 191:122227
36. Arserim-Uçar DK et al (2021) Characterization of bacterial cellulose nanocrystals: Effect of acid treatments and neutralization. Food Chem 336:127597
37. Khor L, Cheong KY (2013) Aloe vera gel as natural organic dielectric in electronic application. J Mater Sci 24:2646–2652
38. Rihayat T et al (2019) Wound dressing based on banana peels waste and chitosan by strengthening lignin as wound healing medicine. IOP Conf Ser Mater Sci. Eng 506:012056
39. Anbazhagan S, Thangavelu KP (2018) Application of tetracycline hydrochloride loaded-fungal chitosan and *Aloe vera* extract based composite sponges for wound dressing. J Adv Res 14:63–71
40. Zahedi P et al (2013) Preparation and release properties of electrospun poly(vinyl alcohol)/poly(ε-caprolactone) hybrid nanofibers: Optimization of process parameters via D-optimal design method. Macromol Res 21(6):649–659
41. Pereira R, Mendes A, Bártolo P (2013) Alginate/Aloe vera hydrogel films for biomedical applications. Procedia CIRP 5:210–215
42. Mat-Shayuti MS, Abdullah MZ, Megat-Yuso PSM (2013) Water absorption properties and morphology of polypropylene/ polycarbonate/polypropylene-graft-maleic anhydride blends. Asian J Sci Res 6:167–176
43. Schindler C et al (2013) Electrospun polycaprolactone/polyglyconate blends: Miscibility, mechanical behavior, and degradation. Polymer 54(25):6824–6833
44. Melnik EV et al (2019) In vitro degradation behaviour of hybrid electrospun scaffolds of polycaprolactone and strontium-containing hydroxyapatite microparticles. Polym Degrad Stab 167:21–32
45. Aydogdu MO et al (2019) Fiber forming capability of binary and ternary compositions in the polymer system: Bacterial Cellulose–Polycaprolactone–Polylactic Acid. Polymers 11(7):1148
46. Carter P, Rahman S, Bhattarai N (2016) Facile fabrication of *Aloe Vera* containing PCL nanofibers for barrier membrane application. J Biomater Sci Polym Ed 27:1–31
47. D Zeleniakienė et al., (2003) The influence of porosity on stress and strain state of porous polymer materials. Kaunas University of Technology, UK
48. Siboro SAP et al (2021) Tunable porosity of covalently crosslinked alginate-based hydrogels and its significance in drug release behavior. Carbohydr Polym 260:117779
49. Isfahani FR, Tavanai H, Morshed M (2017) Release of *Aloe vera* from electrospun aloe vera-PVA nanofibrous pad. Fibers and Polymers 18(2):264–271
50. Song W, Mano JF (2013) Interactions between cells or proteins and surfaces exhibiting extreme wettabilities. Soft Matter 9:2985–2999
51. Ramos DM et al (2019) Insulin immobilized PCL-cellulose acetate micro-nanostructured fibrous scaffolds for tendon tissue engineering. Polym Adv Technol 30(5):1205–1215
52. Zhang J et al (2017) Dual effects of N, N-dimethylformamide on cell proliferation and apoptosis in breast cancer. Dose Response 15:155932581774445
53. Li S, Wang C (2018) Study on the potential way of hepatic cytotoxicity of dimethylformamide. J Biochem Mol Toxicol 32(9):e22190

Authors and Affiliations

Pornsuda Kotcharat[1] · Piyachat Chuysinuan[2] · Thanyaluck Thanyacharoen[2] · Supanna Techasakul[2] · Sarute Ummartyotin[1]

[1] Faculty of Science and Technology, Department of Materials and Textile Technology, Thammasat University, Pathumthani, Thailand

[2] Laboratory of Organic Synthesis, Chulabhorn Research Institute, Bangkok, Thailand